$Rb[Li_5Si_2O_7]$ – A Latecomer in the Family of Alkali Lithosilicates Hiding a Green-Emitting Lithosilicate

Freia Ruegenberg,[a] Markus Seibald,[b] Dominik Baumann,[b] Simon Peschke,[b] Frauke Philipp,[b] and Hubert Huppertz*[a]

Abstract: In order to expand the field of alkali lithosilicates, a new representative of the substance class with a previously unknown structure type was found based on solid-state synthesis. The novel compound with the sum formula $Rb[Li_5Si_2O_7]$ crystallizes in the orthorhombic space group *Pbcm* (no. 57) with $a = 7.6269(3)$, $b = 9.5415(4)$, and $c = 9.4095(3)$ Å by means of single-crystal X-ray diffraction. The structure consists of a highly condensed lithosilicate framework, built up of corner- and edge-linked $[LiO_4]$-tetrahedra and $[Si_2O_7]$-units, and the rubidium ions aligned in channels. Suitable crystals of the material were obtained using sealed tantalum ampoules as reaction tube at a temperature of 750 °C. The new compound was further characterized via powder diffraction, Rietveld analysis, and EDX measurements. At first glance, Eu^{2+}-doped $Rb[Li_5Si_2O_7]$ reveals an intense green luminescence. In-depth crystal analysis shows that a core-shell formation is present even for apparently high quality single-crystals. As a minority phase, the known green phosphor $RbLi[Li_3SiO_4]_2:Eu^{2+}$ is the origin of the luminescence, representing a tiny core inside of the particles surrounded by a large matrix of transparent $Rb[Li_5Si_2O_7]$ dominating the single-crystal diffraction pattern.

Introduction

Alkali lithosilicates have already been investigated and described in detail in the 1980s, especially by the working group around Rudolf Hoppe. The syntheses at that time were mainly based on the alkali metal oxides and were carried out in sealed nickel ampoules over a reaction time of several days or weeks. Quite a number of alkali lithosilicates were discovered this way, namely $K[Li_3SiO_4]$,[1] $Rb_2[Li_2SiO_4]$,[2] $Na[Li_3SiO_4]$,[3] $K_3[LiSiO_4]$,[4] $RbLi[Li_3SiO_4]_2$,[5] $RbNa[Li_3SiO_4]_2$, $RbNa_3[Li_3SiO_4]_4$, $CsKNa_2[Li_3SiO_4]_4$, $CsKNaLi[Li_3SiO_4]_4$,[6] and $Cs_2[Li_2SiO_4]$.[7] Common feature of all these compounds is an anionic framework of interconnected $[LiO_4]$- and $[SiO_4]$-tetrahedra, in which the cations with higher coordination numbers are embedded. In all of them, silicon and lithium act as framework builders, which is why they are classified as lithosilicates.

In the light of the invention and development of LEDs and the search for new, efficient phosphors, alkali lithosilicates recently re-entered the researchers focus. For quite a long time, the suitability of alkali compounds as host lattices for Eu^{2+} was considered impossible, because for example charge balancing in the structure was thought to be unfeasible. The successful doping of an alkali lithosilicate was first reported by Dutzler et al. in 2018 with $Na[Li_3SiO_4]:Eu^{2+}$, $NaK_7[Li_3SiO_4]_8:Eu^{2+}$ and $K[Li_3SiO_4]:Eu^{2+}$ as examples.[8] A whole series of new releases about alkali lithosilicates was published since then, largely describing the successful doping with Eu^{2+} of already known alkali lithosilicates.[9] However, in the course of this development, some previously unknown alkali lithosilicates have also been discovered and characterized.[9e,10]

Most of the above-mentioned alkali lithosilicates crystallize in the UCr_4C_4-structure type (*I*4/*m*, no. 87) or a structurally related variant of this type. Their common characteristic structural feature are endless channels extending along a crystallographic axis in the highly condensed anionic framework of vertex- and edge-sharing $[LiO_4]$- and $[SiO_4]$-tetrahedra. Depending on the extent and manner in which channels are formed and occupied by the different alkali-metal cations, different structural variants with varying space groups result.

A majority of the previously known alkali lithosilicates exhibit the space group *I*4/*m* and can be described with the general formula $A_4[Li_3SiO_4]_4$. Depending on the exact composition, up to four of the alkali metal cations Li^+, Na^+, K^+, Rb^+, and Cs^+ can be located in the channels built up by the lithosilicate framework, which forms a so–called *vierer*[11] ring structure.

In the space group $I4_1/a$ (no. 88), there are the two alkali lithosilicates $Na[Li_3SiO_4]$ and $NaK_7[Li_3SiO_4]_8$, representing a structure variant of the UCr_4C_4-structure type.

Only two compounds have been described so far in the monoclinic space group *C*2/*m* (no. 12), namely $RbNa[Li_3SiO_4]_2$ and $RbLi[Li_3SiO_4]_2$. Same as the structural variants in *I*4/*m* and

[a] F. Ruegenberg, Prof. Dr. H. Huppertz
Institut of Gerneral, Inorganic, and Theoretical Chemistry
University of Innsbruck
Innrain 80–82, 6020 Innsbruck (Austria)
E-mail: Hubert.Huppertz@uibk.ac.at
Homepage: https://www.uibk.ac.at/aatc/mitarbeiter/hub/

[b] Dr. M. Seibald, Dr. D. Baumann, Dr. S. Peschke, Dr. F. Philipp
OSRAM Opto Semiconductors GmbH
Mittelstetter Weg 2, 86830 Schwabmünchen (Germany)

Supporting information for this article is available on the WWW under https://doi.org/10.1002/chem.202101433

$I4_1/a$, the lithosilicate framework forms *vierer* ring channels, in this case occupied by Rb^+ and either Na^+ or Li^+.

The only alkali lithosilicate known to date that crystallizes in the space group $P2_1/c$ (no. 14) is $K_3[LiSiO_4]$. Again, the higher coordinated cations K^+ are embedded in a lithosilicate framework, but channels are no longer visible, thus it is not considered as a UCr_4C_4-structure type variant.

Within the space group $P\bar{1}$, finally, the compounds $K[Li_3SiO_4]$, $Rb_2[Li_2SiO_4]$, and $Cs_2[Li_2SiO_4]$ are known.

While $K[Li_3SiO_4]$ also forms characteristic *vierer* ring channels filled with K^+, such a structural motif is no more evident in $Rb_2[Li_2SiO_4]$ and $Cs_2[Li_2SiO_4]$. For this reason, the last two also belong to the exceptions that are not described as related to the UCr_4C_4-structure type.

After the first comprehensive studies of Hoppe and a large amount of recent research results, one might think that the structural variety of alkali lithosilicates has already been fully investigated. Nevertheless, here we report about a so far unknown alkali lithosilicate. Even though the new compound with the formula $Rb[Li_5Si_2O_7]$ displays a few structural analogies to the already known alkali lithosilicates, it shows a completely new, hitherto unknown structure type, which will be described in this article.

Table 1. Crystallographic data of the single-crystal refinement of $Rb[Li_5Si_2O_7]$.

Parameter	Value
Empirical formula	$RbLi_5Si_2O_7$
Molecular weight /g mol^{-1}	288.35
Crystal system	orthorhombic
Space group	*Pbcm* (no. 57)
Diffractometer	Bruker D8 QUEST PHOTON 100
Radiation; wavelength /Å	Mo-Kα; 0.71073
a /Å	7.6269(3)
b /Å	9.5415(4)
c /Å	9.4095(3)
Cell volume /Å^3	684.75(5)
Formula units per unit cell	4
Calculated density /g cm^{-3}	2.797
Temperature /K	299(2)
Absorption coefficient /mm^{-1}	7.57
F(000) /e	544
Profile range /deg	5.34–78.61
Index ranges /*hkl*	$-12<h<12$; $-15<k<15$; $-15<l<15$
Total reflections	31073
Independent reflections	1519
R_{int}	4.29
Reflections with $I>2\sigma(I)$	1519
R_σ	1.64
Data/ref. parameters	1757/79
Absorption correction	multi-scan (SADABS-2016/2)[12]
Goodness-of-fit on F^2	1.048
Final *R*1/*wR*2 [$I>2\sigma(I)$]	0.0188/0.0400
*R*1/*wR*2 indices (all data)	0.0261/0.0418
Largest diff. peak/hole /e Å^{-3}	0.60/−0.61

Results and Discussion

Initial syntheses targeting new doped variants of alkali lithosilicates yielded a product, which exhibited unexpected reflections in the resulting powder pattern. Thus, single-crystals were isolated, among them one of the new compound.

Once the empirical formula $Rb[Li_5Si_2O_7]$ was determined via single-crystal structure solution and refinement, attempts could be made to selectively synthesize crystals of the new phase, whereby the hitherto most efficient route is described in the Experimental Section.

In order to investigate the suitability of the new alkali lithosilicate as a phosphor, the syntheses were performed with a dopant amount of 1 mol% europium.

Subsequently, the products were analyzed by single-crystal and powder X-ray diffraction (SCXRD/ PXRD), as well as energy-dispersive X-ray (EDX) spectroscopy. Structure solution and refinement based on single-crystal data of the new compound $Rb[Li_5Si_2O_7]$ were performed in the orthorhombic space group *Pbcm* (no. 57) with unit cell metrics of $a=7.6269(3)$, $b=9.5415(4)$, and $c=9.4095(3)$ Å. The crystallographic data of the compound crystallizing in the new structure type can be found in Table 1. Although the structure differs in some significant respects, there are also parallels that can be drawn towards the other alkali lithosilicates.

First of all, just like for the UCr_4C_4-type alkali lithosilicates, a highly condensed lithosilicate framework is present in the new compound, offering space for the higher coordinated alkali metal cation Rb^+. The degree of condensation of the lithosilicate framework κ is 1 for both the new compound and the UCr_4C_4-type alkali lithosilicates, describing the atomic ratio (Li, Si) : O. However, in contrast to all previously described alkali lithosilicates, in this case the $[SiO_4]$-tetrahedra in the lithosilicate framework are not isolated from each other (Figure 1a). There are two crystallographically distinguishable Si^{4+}-sites Si1 (ligands: 2×O1, O3, O5) and Si2 (ligands: O4, 2×O2, O5), whose coordination tetrahedra are linked via a shared oxygen vertex (Figure 1b), forming $[Si_2O_7]$-disilicate units. The Si–O bond lengths within the tetrahedra vary between 1.598(1) and 1.684(1) Å, and fit well to those known from the literature.[11] Exact values and details can be found in the Supporting Information. The disilicate units themselves are isolated from each other, linked only by $[LiO_4]$-tetrahedra. Concerning these, three different Li sites can be distinguished. Li1 and Li2 are located on general positions and $[LiO_4]$-tetrahedra of each form endless strands along the crystallographic *c*-axis, whereas two edge-linked double tetrahedra units are bridged together via a common oxygen (O3 for Li1 respective O4 for Li2). At the shared oxygen vertex between the bridged Li2 double tetrahedra, the tetrahedra from the general Li3 position are linked via common edges (Figure 1d). Due to the 2_1-screw axis parallel to *b*, each of these units is shifted by *b*/2 and rotated by 180° regarding to the preceding unit. In sum, this results in a layer-like substructure of $[LiO_4]$-tetrahedra meandering along parallel to the crystallographic *b*-axis (Figure 1 c). These $[LiO_4]$-layers, extending endlessly perpendicular to the [100]-axis, are interconnected via the $[Si_2O_7]$-units, sharing common vertexes (O1 and O3) (see Figure 2).

With respect to the $[LiO_4]$-tetrahedra, such a dense linkage via common vertexes and edges is known from the two isotypic alkali lithosilicates $Cs_2[Li_2SiO_4]$ and $Rb_2[Li_2SiO_4]$, as well as in $K[Li_3SiO_4]$. However, $Cs_2[Li_2SiO_4]$ and $Rb_2[Li_2SiO_4]$ exhibit a lower

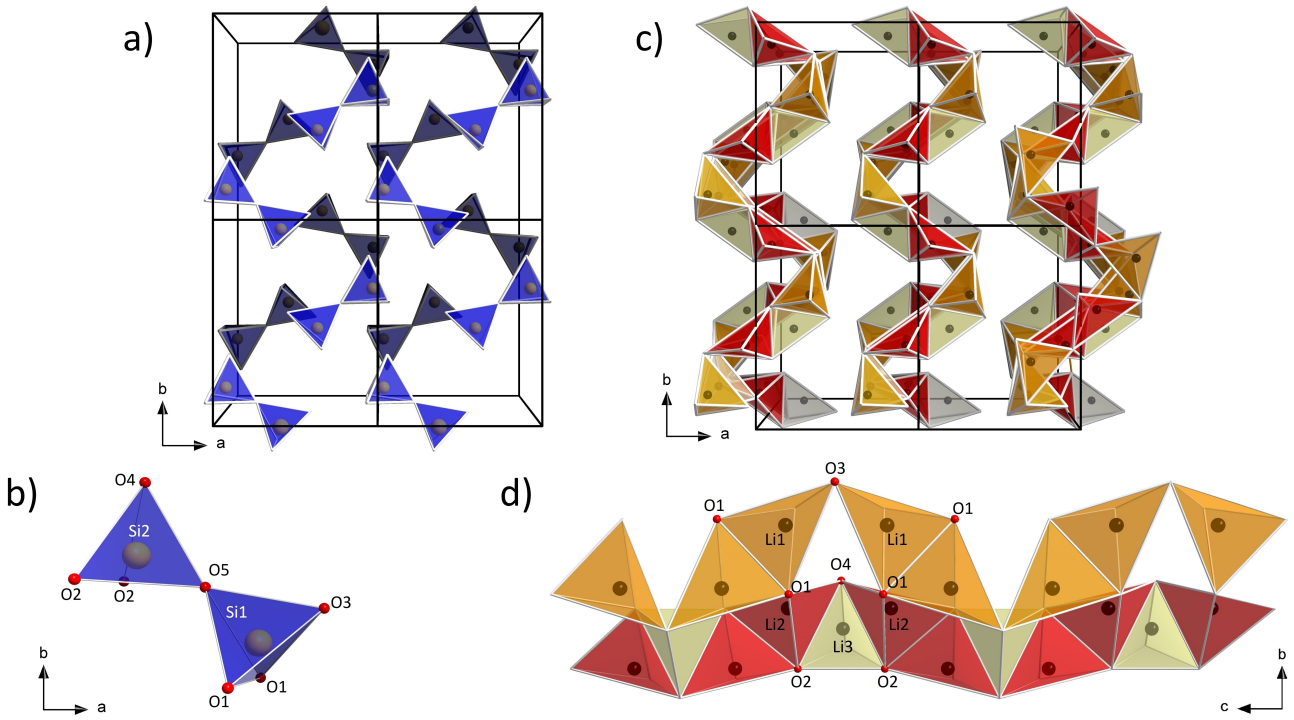

Figure 1. Illustration of the lithosilicate framework's structure in $Rb[Li_5Si_2O_7]$: in a), a quadruple cell along [00$\bar{1}$] is shown with the $[Si_2O_7]$-double tetrahedra units isolated from each other, while in b) such a unit is shown in detail. Figure 1c) illustrates the $[LiO_4]$-tetrahedra linkage, showing the three different $[LiO_4]$-tetrahedra representing the three independent Li sites in different colors (Li1 orange, Li2 red, Li3 beige). In d), a detailed view of a section of the $[LiO_4]$-connectivity is shown as a strand along [001] with linkage patterns.

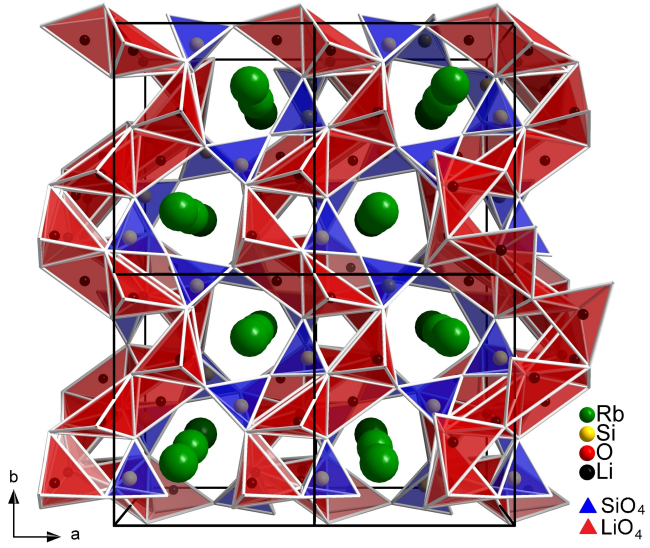

Figure 2. Projection of the overall structure of $Rb[Li_5Si_2O_7]$ as a quadruple cell along [00$\bar{1}$].

degree of condensation of $\kappa = 0.75$ in contrast to $Rb[Li_5Si_2O_7]$. The other highly condensed UCr_4C_4-type alkali lithosilicates with $\kappa = 1$ show an equally corner- and edge-linked system of $[LiO_4]$-tetrahedra, resulting in other structural building blocks. Regarding the linkage of the Li-tetrahedra in UCr_4C_4-type compounds generally, the only exception known so far is the oxonitridolithoaluminate $Sr[Li_2Al_2O_2N_2]$. This compound, which has become known as a high-performance red phosphor (SALON) when doped with Eu^{2+}, is also highly condensed ($\kappa = 1$) and is up to now the only UCr_4C_4-related compound to have only corner-linked $[LiO_3N]$-tetrahedra.[13]

As mentioned above, the presence of $[Si_2O_7]$-disilicate units is so far unique among the alkali lithosilicates. However, the structural motif can be found in group silicate phosphors such as $Ca_2Mg[Si_2O_7]:Eu^{2+}$[14] or in the mixed sorosilicate phosphor $BaY_4Si_5O_{17}:Eu^{2+}$.[15] Furthermore, nitride phosphor materials such as $Ca_3Mg[Li_2Si_2N_6]:Eu^{2+}$,[16] $Li_2Ca_2[Mg_2Si_2N_6]:Eu^{2+}$, and $Ba[Li_2(Al_2Si_2)N_6]:Eu^{2+}$[17] exhibit similar structural motifs by means of highly interconnected tetrahedral frameworks, but in this case with edge-sharing $[Si_2N_6]$-units.

The highly condensed lithosilicate framework in $Rb[Li_5Si_2O_7]$ forms characteristic channels along the crystallographic *c*-axis, known in a comparable way from other alkali lithosilicates. In these channels, which unlike in many of the other alkali lithosilicates cannot be described as *vierer* rings, the rubidium ions are arranged alongside each other. A single rubidium site is present, which is six-fold coordinated by the oxygen ions (2× O1, 2×O5, 2×O4, Figure 3). The bond lengths with 2.914(7), 2.9425(6), and 3.1598(7) Å are close to the theoretically calculated length via the ionic radii of Rb–O in a sixfold coordination of 2.92 Å.[18] The coordination spheres are linked by a common edge, sharing O4 and O5. Additional crystallographic information is available in the Supporting Information (Tables S1–S5).

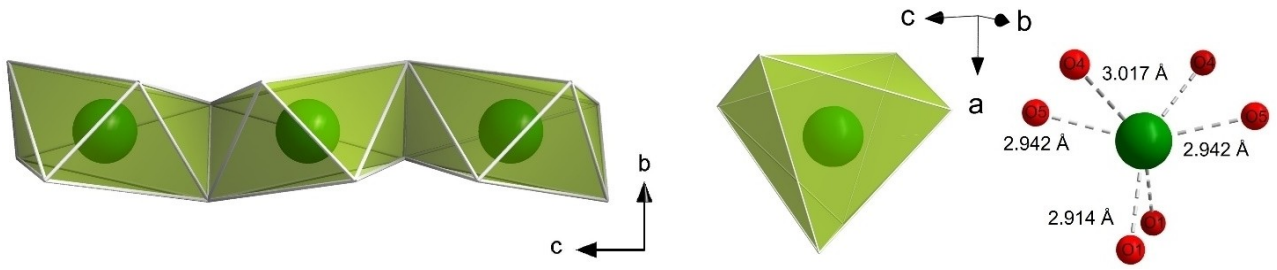

Figure 3. Schematic representation of the strands along [001] of edge-linked distorted six-fold coordination spheres around Rb^+ (green) and detailed image of the coordination environment with Rb–O bond lengths.

In order to furthermore check on the reliability of the determined structure, the bond valences were calculated according to the bond-length/bond-strength (ΣV)[19] and the CHARDI (ΣQ)[20] concept (Table S6). The highest deviations are found in the ΣV-values for Li3 and O3: Li3 with a calculated value of +1.21 is the one Li^+ most deflected from the tetrahedra center and O3 with a value of −1.79 is the only oxygen ion not involved in the primary coordination of Rb^+.

Additionally, the Madelung part of lattice energy (*MAPLE*)[21] was calculated and is in good agreement with the values obtained by subtraction of the *MAPLE*-values of the related compounds $RbLi[Li_3SiO_4]_2$[5] and Li_2O (Table S6).

Syntheses as described in the Experimental Section yielded crystalline powder samples with $Rb[Li_5Si_2O_7]$ as main phase. However, an intense green luminescence ($\lambda_{max} \approx 525$ nm, *fwhm* ≈ 45 nm) was observed, apparently homogeneously distributed throughout the powders, which fits very well to that of the already known compound $RbLi[Li_3SiO_4]_2:Eu^{2+}$.[9c] Unlike in $Rb[Li_5Si_2O_7]$, the $[SiO_4]$-units are isolated from each other in the case of $RbLi[Li_3SiO_4]_2$. Nevertheless, assuming the lithosilicate framework as the basic structure, both can be described as a tectosilicate. They can thus be clearly distinguished structurally from also green luminescent orthosilicates such as $(Sr_{2-x}Ba_x)SiO_4:Eu^{2+}$ where the $[SiO_4]$-units are not at all connected. Classical orthosilicates also differ clearly from highly condensed alkali lithosilicates with respect to the full-widths at half maximum values.[22]

In order to address whether the luminescence could be caused by the secondary phase $RbLi[Li_3SiO_4]_2:Eu^{2+}$ or by $Rb[Li_5Si_2O_7]:Eu^{2+}$ itself, a Rietveld refinement was performed. The results are shown in the Supporting Information as a plot of the powder pattern (Figure S2) and the parameters in Table S7.

The lattice parameters calculated by this method for $Rb[Li_5Si_2O_7]$ with $a = 7.6330(2)$, $b = 9.5578(4)$, and $c = 9.4235(3)$ Å fit very well to those obtained from the single-crystal. With a phase fraction of 74.9(6) wt%, the new compound represents the main component in the powder product. As guessed from the luminescence, $RbLi[Li_3SiO_4]_2$ can indeed be refined as a minor phase component with a fraction of 10.0(4) wt%. As further secondary phase, non-luminescent Li_4SiO_4 with a share of 15.1(6) wt% could be identified. In addition, there is a small number of unassignable residual reflections in the powder pattern of the bulk product.

Remarkably, the green luminescence is not clearly assignable when studying the powder more closely. During the investigation of single-crystals, homogeneously green luminescent individuals were also found, which revealed the cell of the new compound $Rb[Li_5Si_2O_7]$. These crystals were isolated under polarized light, showing an extinction behavior like single-crystals.

Only upon closer examination under a light microscope equipped with an optical filter unit for luminescence analysis, an interesting phenomenon could be observed. The previously isolated crystals were progressively crushed, resulting in the spalling of large pieces of non-luminescent matrix. To these non-luminous fragments, the cell $Rb[Li_5Si_2O_7]$ can be assigned once again by SCXRD. After repeated crushing of the luminescent core fractions, small green emitting particles remained, on which the cell of $RbLi[Li_3SiO_4]$ can be determined, but which no longer can be measured by single-crystal diffraction due to their small size and poor crystallinity. The issue of this core-shell relation is illustrated in Figure 4. The amount of non-luminous transparent matrix is significantly higher than that of the green luminescent component, which, according to the emission can be assigned to $RbLi[Li_3SiO_4]_2:Eu^{2+}$. Nevertheless, tiny cores of this green luminescent secondary phase are sufficient to give a homogeneous green luminescence to a large crystal that appears to be a single-crystal of $Rb[Li_5Si_2O_7]$ according to X-ray diffraction. A detailed size analysis by microscope of the fragments can be found in the Supporting Information in Figure S2.

A large number of synthesis approaches with the same or similar synthesis conditions have been carried out with the aim of obtaining $Rb[Li_2Si_5O_7]$ as a phase-pure product. However, even under apparently identical circumstances, typical minor phases are always formed in varying fractions. There seems to be a synthetic relationship between the new compound $Rb[Li_5Si_2O_7]$ and $RbLi[Li_3SiO_4]_2$, different lithium silicates, and the binary oxides, possibly in the sense of a thermal decomposition or an alternative reaction. Syntheses without doping and without lithium as reducing agent were also performed, but these experiments led to a further reduced phase fraction of $Rb[Li_5Si_2O_7]$ under otherwise identical conditions. Presumably, a flux effect of Eu_2O_3, which may favor the formation of larger

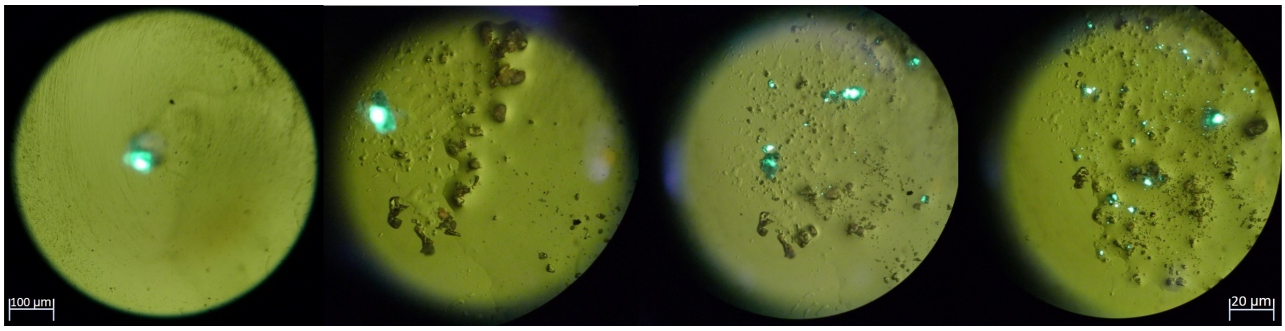

Figure 4. From left to right (increasing magnification, benchmarks for size estimation): Sequential pictures of the fragmentation of a green luminescent crystallite into increasingly smaller fragments under the punctual application of pressure with increase of magnification. Especially in the second image from the left, the large-scale spalling of the transparent matrix can be seen.

crystallites, plays a decisive role in the formation of Rb-$[Li_2Si_5O_7]$.[23] From our observations, we can state that an initial formation of $RbLi[Li_3SiO_4]_2$ could be assumed, followed by a thermal decomposition of the crystallites from the outside to the inside via evaporation of Li_2O, first forming the new compound $Rb[Li_2Si_5O_7]$ as a matrix, and then leading to further decomposition products like the lithium silicates. If smaller crystallites would be formed in the absence of Eu_2O_3, decomposition would also proceed more rapidly and the more complex compounds formed initially would no longer appear in the product. In any case, conducting the experiment under doping conditions has first revealed the core-shell issue. This phenomenon may allow conclusions to be drawn about the formation process of the new compound $Rb[Li_5Si_2O_7]$, that has apparently been overlooked so far in an otherwise very well-studied material system.

To confirm the composition of the new compound, energy dispersive X-ray spectroscopy was performed on crystallites from the powder sample. It should be noted, that the EDX technique cannot be used to distinguish the compound $Rb[Li_5Si_2O_7]$ from the secondary phase $RbLi[Li_3SiO_4]_2$, since the ratio of the cations Rb:Si is 1:2 in both cases, Li is not measurable with this kind of detector and Si/O analysis is not significant within the typical experimental errors of this method, especially under atmospheric storing conditions for the sample. Four different, transparent, non-luminous regions of a crystallite were examined for the measurement. The expected elements Rb, Si and O can be found and when normalized to Rb, a molar ratio Rb:Si of 1:2.2(6) is obtained. The slightly higher calculated contribution from Si can be explained by the weaker excitability of the Rb Kα transition associated with the overlap of Si Kα with the Rb Lα transition. Thus, Rb is accounted for to a lesser extent, and a larger share of the overlap peak is attributed to Si. Taking this into account, it is possible to confirm the elemental ratio of the heavy cations in $Rb[Li_5Si_2O_7]$ by EDX.

Conclusion

In this publication, a new group member of alkali lithosilicates with the sum formula $Rb[Li_5Si_2O_7]$ is described, exhibiting a previously unknown structure type in the space group *Pbcm* (no. 57). Although there are structural similarities to known alkali lithosilicates with interesting emission properties when doped with Eu^{2+}, the compound could not be doped with the methods used so far and is therefore considered unsuitable as a phosphor. One reason for this could be the ordering of the cation positions in the lithosilicate framework. Unlike with other alkali lithosilicates, only one single position is available outside the rigid lithosilicate framework, namely that of the heavy Rb^+. This severely limits the possibility of charge balancing, as is necessary for the incorporation of Eu^{2+}.

Eventual green luminescence observed after synthesis can be assigned to the already known secondary phase $RbLi[Li_3SiO_4]_2$:Eu^{2+}. Also after synthesis variation, it was not possible to obtain phase pure $Rb[Li_5Si_2O_7]$. A presumably more elaborate synthesis optimization could therefore be a goal of future work. Even if barely significantly detectable by X-ray diffraction, $RbLi[Li_3SiO_4]_2$:Eu^{2+} co-crystallizes, often as a tiny core in core-shell particles, on which the secondary phase can primarily be identified on the basis of the intense green luminescence. Diffraction behavior on such "single-crystals" is constantly dominated by $Rb[Li_5Si_2O_7]$ and no signs of significant attachments, false metrics, or twinning emerge. Nevertheless, these apparent "single-crystals" consist of two individuals; therefore, an unrestricted assignment of structure and properties is not possible.

Concluding, despite its unsuitability as a phosphor, the new compound $Rb[Li_5Si_2O_7]$ proves that even well-studied substance classes like the alkali lithosilicates still have surprises to offer and may not have been fully exploited yet.

Experimental Section

Synthesis: Samples of the new compound were prepared by high-temperature solid-state synthesis in sealed tantalum crucibles. For this purpose, the reactants Rb_2CO_3 (37.0 mg, ChemPur, 99.9%), Li_2O (23.9 mg, Alfa Aesar, 99.5), SiO_2 (38.5 mg, Fluka, >99.9%), Eu_2O_3 (1 mol%, 0.6 mg, Smart Elements, 99.9%) and 5 wt.% lithium metal as flux and reducing agent (5.0 mg, Sigma Aldrich, 99%) were stoichiometrically weighed in a glovebox (argon atmosphere, UniLab Plus Glove Box Workstation, MBraun, Garching, Germany).

The compounds were ground under inert gas atmosphere using an agate mortar and transferred into a tantalum ampoule, which was subsequently sealed via argon arc welding. The crucibles were placed in evacuated silica glass ampoules and heated to 750 °C at 3 °C min^{-1} using a tube furnace. After 4 h heating phase, the samples were cooled down with 1.5 °C. The ampoules were opened and the products were further examined under atmospheric conditions. The resulting crystalline powders showed a more or less homogeneously distributed green luminescence under excitation with UV-light, which, however, can be attributed to the secondary phase $RbLi[Li_3SiO_4]_2:Eu^{2+}$. Pure-phase synthesis of $Rb[Li_5Si_2O_7]$ was not achieved using the methods presented here. The products show no detectable decomposition for months under atmospheric conditions.

Single-crystal X-ray diffraction: Crystallographic data of single-crystals of the new compound $Rb[Li_5Si_2O_7]$ were obtained from a Bruker D8 Quest diffractometer (Mo-Kα radiation, $\lambda = 0.71073$ Å; Billerica, USA) equipped with a microfocus X-ray tube (Incoatex, Geesthacht, Germany) combined with a Photon 100 detector. Multi-scan absorption correction of the intensity data and data processing were conducted using the software tools SAINT[24] and SADABS.[25] The structure was solved using Direct Methods provided by SHELXS[26] and refined with SHELXL[27] as implemented in the WinGX[28] suite. Deposition Number 2088624 contains the supplementary crystallographic data for this paper. These data are provided free of charge by the joint Cambridge Crystallographic Data Centre and Fachinformationszentrum Karlsruhe Access Structures service www.ccdc.cam.ac.uk/structures.

Powder X-ray diffraction: A STOE STADI P diffractometer (Mo-$K\alpha_1$ radiation, $\lambda = 0.7093$ Å) with a Ge(111) monochromator and a Mythen 1 K detector in Debye-Scherrer geometry was used to collect powder data from the bulk product. Rietveld refinement for verification of the phase composition and structural parameters was performed using the software Topas 4.2.

EDX spectroscopy and electron microscopy: For further confirmation of the chemical composition, a SUPRA™35 scanning electron microscope (SEM, Carl Zeiss, field emission; Oberkochen, Germany) equipped with a Si/Li EDX detector (OXFORD INSTRUMENTS, model 7426; Abingdon, Great Britain) was used to conduct EDX measurements. A maximum acceleration voltage of 25kV was applied for chemical analysis.

Microscopy: A Leica Microsystems microscope (model M205 FA; Wetzlar, Germany) equipped with a polarization filter and an optical filter (UV/ blue spectral range) with a maximum magnification of 1280 was used for optical evaluation and isolation of the crystals and for the examination and differentiation of the eventual appearing green luminescence. As light source, a Lumen Dynamics (model X-Cite exacte; Ontario, Canada) with a Hg lamp-based emission spectrum was used.

Conflict of Interest

The authors declare no conflict of interest.

Keywords: high-temperature chemistry · luminescence · silicates · solid-state reactions

[1] R. Werthmann, R. Hoppe, *Z. Anorg. Allg. Chem.* **1984**, *509*, 7–22.
[2] R. Hofmann, B. Nowitzki, R. Hoppe, *Z. Naturforsch. B* **1985**, *40*, 1441–1452.
[3] B. Nowitzki, R. Hoppe, *Rev. Chim. Miner.* **1986**, *23*, 217–230.
[4] R. Hofmann, R. Hoppe, *Z. Anorg. Allg. Chem.* **1988**, *560*, 35–46.
[5] K. Bernet, R. Hoppe, *Z. Anorg. Allg. Chem.* **1991**, *592*, 93–105.
[6] J. Hofmann, R. Brandes, R. Hoppe, *Z. Anorg. Allg. Chem.* **1994**, *620*, 1495–1508.
[7] K. Bernet, J. Kissel, R. Hoppe, *Z. Anorg. Allg. Chem.* **1991**, *593*, 17–34.
[8] a) D. Dutzler, M. Seibald, D. Baumann, H. Huppertz, *Angew. Chem. Int. Ed.* **2018**, *57*, 13676–13680; b) M. Seibald, D. Baumann, T. Fiedler, S. Lange, H. Huppertz, D. Dutzler, T. Schröder, D. Bichler, G. Plundrich, S. Peschke, G. Hoerder, G. Achrainer, K. Wurst (OSRAM Opto Semiconductors GmbH), WO/2018/029304, **2018**.
[9] a) M. Iwaki, S. Kumagai, S. Konishi, A. Koizumi, T. Hasegawa, K. Uematsu, A. Itadani, K. Toda, M. Sato, *J. Alloys Compd.* **2019**, *776*, 1016–1024; b) H. Liao, M. Zhao, M. S. Molokeev, Q. Liu, Z. Xia, *Angew. Chem.* **2018**, *130*, 11902–11905; c) M. Zhao, H. Liao, L. Ning, Q. Zhang, Q. Liu, Z. Xia, *Adv. Mater.* **2018**, *30*, 1802489; d) M. Liao, Z. Mu, Q. Wang, X. Zhang, H. Dong, M. Wen, F. Wu, *J. Alloys Compd.* **2020**, 155084; e) M. Zhao, Y. Zhou, M. S. Molokeev, Q. Zhang, Q. Liu, Z. Xia, *Adv. Opt. Mater.* **2019**, *7*, 1801631; f) L. Wang, X. Kong, P. Li, W. Ran, X. Lan, Q. Chen, J. Shi, *Inorg. Chem. Front.* **2019**, *6*, 3604–3612.
[10] a) M. Zhao, H. Liao, M. S. Molokeev, Y. Zhou, Q. Zhang, Q. Liu, Z. Xia, *Light-Sci. Appl.* **2019**, *8*, 38; b) D. Dutzler, M. Seibald, D. Baumann, F. Philipp, S. Peschke, H. Huppertz, *Z. Naturforsch. B* **2019**, *74*, 535–546; c) F. Ruegenberg, M. Seibald, D. Baumann, S. Peschke, P. C. Schmid, H. Huppertz, *Chem. Eur. J.* **2020**, *26*, 2204.
[11] F. Liebau in *Structural Chemistry of Silicates*, Springer, Berlin, Heidelberg, **1985**.
[12] G. M. Sheldrick, SADABS, v2014/5, Bruker AXS Inc., Madison, WI, USA, **2001**.
[13] G. J. Hoerder, M. Seibald, D. Baumann, T. Schröder, S. Peschke, P. C. Schmid, T. Tyborski, P. Pust, I. Stoll, M. Bergler, C. Patzig, S. Reißaus, M. Krause, L. Berthold, T. Höche, D. Johrendt, H. Huppertz, *Nat. Commun.* **2019**, *10*, 1824.
[14] J. Liu, Y.-T. Wang, C.-Y. Lin, C.-F. Yang, *Cryst. Growth Des.* **2020**, *20*, 3154–3162.
[15] C. Cozzan, G. Laurita, R. Seshadri, in *Abstracts of Papers, 251st ACS National Meeting & Exposition*, San Diego, CA, United States, **2016**.
[16] C. Poesl, W. Schnick, *Chem. Mater.* **2017**, *29*, 3778–3784.
[17] T. M. Tolhurst, P. Strobel, P. J. Schmidt, W. Schnick, A. Moewes, *J. Phys. Chem. C* **2017**, *121*, 14296–14301.
[18] N. Wiberg, E. Wiberg, A. Holleman, in *Lehrbuch der Anorganischen Chemie*, De Gruyter, Berlin, **2007**, p. 2002.
[19] a) N. Brese, M. O'Keeffe, *Acta Crystallogr. Sect. B* **1991**, *47*, 192–197; b) D. Altermatt, I. Brown, *Acta Crystallogr. Sect. B* **1985**, *41*, 240–244.
[20] R. Hoppe, S. Voigt, H. Glaum, J. Kissel, H. P. Müller, K. Bernet, *J. Less-Common Met.* **1989**, *156*, 105–122.
[21] a) R. Hoppe, *Angew. Chem. Int. Ed. Engl.* **1966**, *5*, 95–106; b) R. Hoppe, *Angew. Chem. Int. Ed. Engl.* **1970**, *9*, 25–34; c) R. Hübenthal, *University of Gießen, Germany* **1993**.
[22] a) I. Baginskiy, R. Liu, C. Wang, R. Lin, Y. Yao, *J. Electrochem. Soc.* **2011**, 158, P118; b) S. Poort, W. Janssen, G. Blasse, *J. Alloys Compd.* **1997**, 260, 93–97.
[23] M. Zeuner, F. Hintze, W. Schnick, *Chem. Mater.* **2009**, *21*, 336–342.
[24] Bruker SAINT, v8.34a, Bruker AXS Inc., Madison, WI, USA, **2014**.
[25] L. Krause, R. Herbst-Irmer, G. M. Sheldrick, D. Stalke, *J. Appl. Crystallogr.* **2015**, *48*, 3–10.
[26] G. M. Sheldrick, *Acta Crystallogr. Sect. A* **2008**, *64*, 112–122.
[27] G. M. Sheldrick, *Acta Crystallogr. Sect. C* **2015**, *71*, 3–8.
[28] L. J. Farrugia, *J. Appl. Crystallogr.* **2012**, *45*, 849–854.

Manuscript received: April 21, 2021
Accepted manuscript online: June 10, 2021
Version of record online: July 2, 2021

